

Operating Fiber Networks in the Quantum Limit

Janis Nötzel^{1*†} and Matteo Rosati^{2*†}

¹Emmy-Noether Gruppe Theoretisches Quantensystemdesign
Lehrstuhl für Theoretische Informationstechnik
Technische Universität München.

²Departament de Física: Grup d'Informació Quàntica,
Universitat Autònoma de Barcelona, Bellaterra (Barcelona),
ES-08193, Spain.

*Corresponding author(s). E-mail(s): janis.notzel@tum.de;
matteo.rosati@uab.cat;

[†]These authors contributed equally to this work.

Abstract

We consider all-optical network evolution from a quantum perspective. We show that a use of optimal quantum receivers allows an estimated **55%** decrease in energy consumption of all-optical amplifiers in network configurations that are typical today. We then compare data transmission capacities of quantum receivers with today's technology operating within the boundaries set by Shannon. We find that quantum receiver technology allows for a logarithmic scaling of the system capacity with the baud-rate, while Shannon-type systems are limited by the transmit power. Thus a natural quantum limit of classical data transmission emerges. Based on the above findings we argue for a new approach to optical communication network design, wherein in-line amplifiers are replaced by novel fiber supporting high spectral bandwidth to allow for noiseless data transmission in the quantum limit.

Keywords: Optical networks, Green communication, Quantum communication, Joint detection receiver

1 Introduction

With this work we point out one possible near-term contribution of quantum information processing techniques to existing and near-term data transmission networks, focusing in particular on fiber networks. For the existing networks we focus on quantum receiver technology as a tool for reducing energy consumption in amplifiers. For future networks we explain how amplifiers could be avoided by utilizing the scaling law of the fiber link capacity with the baud-rate when quantum detection methods are used.

1.1 Energy Savings in Current Networks

The progressive development of fiber networks is a driver of productivity growth in modern societies [1]. As a result, network electricity consumption has been estimated as $\approx 1.7\%$ of the global consumption, with a growth rate of $\approx 10\%$ per year [2] in 2012. Thus, energy efficiency has become a key network design principle and one of the main motivations to switch from electrical to optical information-processing in networks, e.g., via the introduction of integrated-photonics circuits [3]. Interestingly, such circuits are also one of the major candidate platforms for quantum information processing (QIP), a field which has long promised to boost the capabilities of classical information technology [4, 5].

However, the potential advantages of QIP for classical data transmission reported so far can be described as “large gains at small practical value”, e.g., the reduction of peak signal energy for deep-space communication and the increase of transmission rate in short-distance communication [6–11].

In this work we change such perspective, proving that QIP can provide a significant reduction of energy consumption in classical-data-transmission systems that employ optical amplification, until even the hypothetical removal of the amplifiers. Optical amplification is a widespread system design, wherein amplifiers are placed along the path to counteract propagation losses that progressively reduce the signal’s strength, ensuring that information can be reliably decoded by the receiving side [12–15]. Such amplifiers consume a considerable amount of energy, e.g., for a 1100 km-link their cost is estimated as $\approx 13\%$ of the total energy consumption [14]; hence a reduction of their energy budget is a worthy objective.

In this setting, we first show that a current communication system employing a quantum optimal joint-detection receiver (OJDR)[16–22] can transfer the same amount of bits of a classical optimal single-symbol receiver (OSSR) by spending less energy per signal, thanks to a net reduction of the amplification costs. The difference between these two receiver designs lies in the way they manipulate the signals: the OSSR performs individual operations on each received signal, thereby immediately producing a classical measurement outcome per pulse; in contrast, the OJDR can perform any collective operation on a long sequence of received signals prior to producing its measurement outcome. Therefore, our results harness the OJDR’s superior capability of reading

off the transmitted data, which is particularly pronounced for signals with low added noise, by extracting the same amount of information from signals of lower energy with respect to an OSSR.

We start by providing a heuristic motivation for the reduction of the amplification costs, based on a striking result: in a quantum communication system employing OJDR, the strategy of turning on all the available amplifiers can be sub-optimal, contrarily to what happens for an OSSR. This property, which favours lower added noise at the cost of a smaller signal amplification, can be used to reduce the amplification energy budget while increasing the communication rate.

We then refine our analysis by considering tunable amplifier gains, which measure the strength of the amplification process and can be related to its energy cost. We formulate the problem of minimizing the total energy cost with respect to the gain profile with OJDR, while attaining a larger communication rate than the OSSR. We provide an algorithm to solve this problem and employ it to predict the maximum reduction of energy consumption in a wide range of distances and numbers of amplifiers.

We show that energy savings arising from the use of an OJDR can be as large as $\approx 100\%$. However, this happens only in settings where the communication system benefits very little from the use of amplifiers in the first place. Instead, in the practically relevant setting where the amplifiers enhance the data-rate at least by a factor of 2, we identify situations where the use of an OJDR allows record energy savings up to $\approx 55\%$.

To the best of our knowledge, the minimization of energy consumption of amplifiers through OJDR technology has been analyzed only in a couple of recent works, though from different perspectives: [11] reported a constant increase of the communication rate using the OJDR instead of the OSSR on an optically-amplified multi-span link; whereas [10] studied the energy-efficiency of a system employing continuous amplification in the limit where the OSSR approximates the OJDR, which fails to capture the full advantage of the OJDR. We combine both approaches to quantify the energy-efficiency advantage of the OJDR on a multi-span optically-amplified link.

1.2 Future Quantum Data Networks

Finally, we provide a theoretical justification for a novel approach to future data transmission network design and detail the first implementable steps to its realization. To this purpose, we point out the strikingly different growth of data transmission capacities of both OSSR and OJDR system-design approaches: under any power limit and any thermal noise level, measured in photons per second, the link capacity grows unbounded with a logarithmic dependence on the baud-rate when an OJDR is used as the receiver. In sharp contrast, the link capacity is upper-bounded in terms of the transmit power when an OSSR is used. Our technological hypotheses can be tested with novel system design concepts resting on the works of Guha et al. [8, 18] and follow-up works of

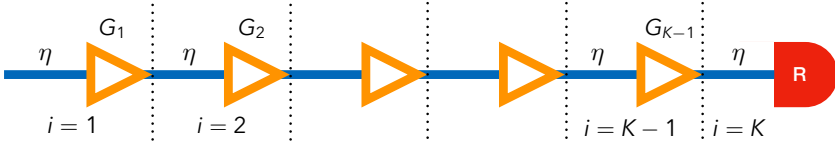


Fig. 1 Depiction of the communication system studied: the optical-fiber link is divided into K segments interleaved by optical amplifiers. Classical information is encoded in a quantum state and sent on the channel. Transmission on each segment i is modelled by a pure-loss bosonic channel of attenuation η followed by a quantum-limited bosonic amplifier channel of gain G_i . The last segment does not benefit from amplification and it is followed by a receiver R that extracts the classical message from the received state. We show that, by using a quantum receiver, one can reduce the amplifier gains and thus spare significant amounts of energy to transfer the same amount of information with respect to a classical receiver.

Rosati et al. [9] and Klimek et al. [23]. For the optical transmission medium, we suggest hollow-core fiber [24, 25].

2 Results

2.1 Communication System Model

Consider a multi-span transmission line comprising an optical-fiber link of length L and K optical-amplifier modules placed at equally spaced intervals of length L/K ¹ (see Figure 1). Each of these components is modelled by a quantum bosonic Gaussian channel, taking as input a quantum state of the electromagnetic field. For such channels, the maximum information transmission rate can be attained by encoding classical information into sequences of optical coherent states [26–28] and performing a collective quantum measurement of the received sequences, to recover the classical message [16–22, 29].

For our purposes, the action of each transmission-line component can be described in terms of input-output relations for the mean energy of the field comprised of signal and noise²:

- (i) transmission on an optical-fiber segment is modelled by a pure-loss channel,

$$n \mapsto \eta \cdot n, \quad (1)$$

with $\eta := e^{-\alpha \frac{L}{K}}$ and $\alpha \geq 0$ a system-specific coefficient;

- (ii) optical amplification is modelled by a quantum-limited amplifier channel,

$$n \mapsto G \cdot n + G - 1, \quad (2)$$

¹The techniques we develop can be applied to amplifiers with arbitrary spacing. Since this does not mark any qualitative change in our results, we restrict to equal spacing for simplicity.

²Throughout the main text, except in Results 2.4, we set $\hbar\omega = 1$ for some fixed signal frequency ω , effectively equating the mean energy of the field with its mean number of photons.

with $G \geq 1$ the amplifier gain and $G - 1$ the minimum photon-noise addition allowed by quantum mechanics.

The action of the entire transmission line is then obtained by repeatedly applying these two channels: at the end of the i -th segment, the input plus noise to the next segment has energy $\tau_i \cdot n + \nu_i$, with

$$\tau_i = G_i \cdot \eta \cdot \tau_{i-1}, \quad \nu_i = G_i \cdot \eta \cdot \nu_{i-1} + G_i - 1, \quad (3)$$

and initial values $\tau_0 = 1$, $\nu_0 = 0$. The resulting coefficients for the entire transmission line are $\tau := \tau_K$, $\nu := \nu_K$.

Communication performance is quantified via the spectral efficiency (SE), i.e., the maximum number of bits transmittable per unit time and frequency, which in our narrowband case coincides with the channel capacity. Importantly, depending on the receiver's capabilities, this quantity can take two different values³: the Shannon SE [30], attainable by performing heterodyne detection on each received signal,

$$S_{\text{sh}}(n, \{G_i\}_{i=1}^K) := \log \left(1 + \frac{\tau \cdot n}{1 + \nu} \right), \quad (4)$$

and the Holevo SE [29, 31], attainable by performing a collective quantum measurement (i.e., the OJDR for this channel) on the received sequences,

$$S_{\text{ho}}(n, \{G_i\}_{i=1}^K) := g(\tau \cdot n + \nu) - g(\nu), \quad (5)$$

where $g(x) := (x + 1) \log(x + 1) - x \log x$.

We stress that the realization of a collective measurement that attains (5) is still an open problem in quantum information theory, with several theoretical proposals that we refer to as OJDR [16–22]. Specifically, the all-optical Hadamard receiver can approximate the OJDR for low received signal energy [8, 9] and no noise, but it is unknown whether a broader class of optical receivers can implement the OJDR in general [32–36]. On the other hand, (4) is attained with an explicit receiver design, which coincides with the OSSR for this channel in the practically relevant regime $\tau \cdot n \gtrsim 2$ [35, 37]. For completeness, in Methods 5.4 we study the performance of the homodyne receiver as well, which coincides with the OSSR for $\tau \cdot n \lesssim 2$, observing an energy-advantage of OJDR also in this case.

2.2 Maximizing spectral efficiency: more data with less amplification

We are now interested in maximizing the SE's (4,5) with respect to the amplifier gains. Following the approach taken in [11], we assume that an energy constraint is imposed on the entire communication link, such that the energy

³Throughout the article the logarithms are taken in base 2.

of the field at any point along the link stays below a threshold:

$$\tau_i \cdot n + \nu_i \leq n_{\max} \quad \forall i = 1, \dots, K. \quad (6)$$

The value of n_{\max} can be determined by practical constraints; in particular we will focus on the case where the sender produces signals of maximum energy, i.e., $n = n_{\max}$. In the following we study the problem of spectral-efficiency-optimal gain selection (SEGS):

$$\begin{aligned} S^{\text{op}}(n) &:= \underset{\{G_i\}_{i=1}^K \in \mathbb{R}^K}{\text{maximize}} \quad S(n, \{G_i\}_{i=1}^K) \\ &\text{subject to : } G_K = 1, 1 \leq G_i \leq G_{\max} \quad \forall i, \\ &\quad \tau_i \cdot n + \nu_i \leq n_{\max} \quad \forall i = 1, \dots, K, \end{aligned} \quad (7)$$

where S is either the Shannon or Holevo SE and the corresponding problems are called Shannon-SEGS and Holevo-SEGS. Let us note that the last amplifier can always be turned off, i.e., $G_K = 1$. Indeed, this amplifier simply constitutes an additional channel acting after the signal is received; hence, by the data-processing inequality, it cannot increase the overall spectral efficiency.

For the Shannon-SEGS, the optimal amplification strategy is simply to turn on all the remaining amplifiers at the maximum value of the gain allowed by the energy constraint (6):

$$G_{i < K} = G_{\max} := \frac{1 + n}{1 + \eta \cdot n} \quad \forall i < K. \quad (8)$$

This follows from the fact that the Shannon SE (4) is a monotonically increasing function of G_i for all $i < K$ (see Methods 5.1.2). The resulting optimal Shannon SE is

$$S_{\text{sh}}^{\text{op}}(n) = \log \left(1 + \frac{\tau_{\max} \cdot n}{1 + (\eta - \tau_{\max}) \cdot n} \right), \quad \tau_{\max} = \eta^K \cdot (G_{\max})^{K-1}. \quad (9)$$

On the other hand, the Holevo-SEGS amplification strategy can be considerably different, due to the presence of a quantum OJDR. In this case, the optimization depends non-trivially on the system parameters η , K and on the input signal energy n . Still, it can be shown that the optimal sequence of gains is non-increasing with i ; indeed, if two gains are in increasing order, switching them always decreases the noise ν in the overall channel without changing its amplification coefficient τ (see Methods 5.1.1). This property, together with the well-known fact that the Holevo SE is never smaller than the Shannon SE [29, 31] leads us to the conclusion that

$$S_{\text{ho}}^{\text{op}}(n) \geq S_{\text{ho}}(n, \{G_{i < K} = G_{\max}, G_K = 1\}) \geq S_{\text{sh}}^{\text{op}}(n). \quad (10)$$

Moreover, in Methods 5.1.3 we prove that the first inequality can be strict, i.e., there exists a whole range of system parameter values such that setting

maximum gains results in a sub-optimal value of S_{ho} and, in fact, a certain number of amplifiers can even be turned off.

We thus conclude that, in general, starting from a fully-amplified link with OSSR, the introduction of an OJDR allows to decrease amplifier gains while increasing the spectral efficiency. In turn, since smaller gains imply a smaller energy consumption to operate the amplifiers, the OJDR allows to spare a certain amount of energy. This motivates taking a comparative look at energy-optimal gain selection for OJDR versus OSSR.

2.3 Minimizing amplifier energy consumption: Problem definition

Every amplifier needs to use up at least the amount of energy that it adds to the incoming field, hence the total amplification energy consumption is at least

$$E(n, \{G_i\}_{i=1}^K) = \sum_{i=1}^K (G_i - 1)(\eta(\tau_{i-1}n + \nu_{i-1}) + 1). \quad (11)$$

A fully-amplified link with OSSR attains SE $S_{\text{sh}}^{\text{op}}(n)$ with an energy consumption of $E_{\text{sh}} := (K-1)(1-\eta)n$. Using the former as a baseline, we can then define the following energy-optimal gain selection (EGS) problem for a transmission link with OJDR:

$$\begin{aligned} E_{\text{egs}} &:= \underset{\{G_i\}_{i=1}^K \in \mathbb{R}^K}{\text{minimize}} \quad E(n, \{G_i\}_{i=1}^K) \\ &\text{subject to : } G_K = 1, 1 \leq G_i \leq G_{\text{max}} \quad \forall i, \\ &\quad S_{\text{ho}}(n, \{G_i\}_{i=1}^K) \geq S_{\text{sh}}^{\text{op}}(n). \end{aligned} \quad (12)$$

Importantly, note that the energy needed to provide a given gain G_i depends on all previous gains $G_{j < i}$ and on the attenuation per segment η . In particular, as the noise added by previous amplifiers increases, so does the energy cost for providing a certain gain. This implies that monotonically decreasing gains are not necessarily optimal for EGS.

We therefore also consider a relaxation of EGS (REGS):

$$\begin{aligned} E_{\text{regs}} &:= \underset{\{G_i\}_{i=1}^K \in \mathbb{R}^K}{\text{minimize}} \quad E'(n, \{G_i\}_{i=1}^K) \\ &\text{subject to : } G_K = 1, 1 \leq G_i \leq G_{\text{max}} \quad \forall i, \\ &\quad S_{\text{ho}}(n, \{G_i\}_{i=1}^K) \geq S_{\text{sh}}^{\text{op}}(n), \end{aligned} \quad (13)$$

Here the energy cost for each amplifier is overestimated as the maximum one, via (6), i.e.,

$$E'(n, \{G_i\}_{i=1}^K) = \sum_{i=1}^K (G_i - 1)(\eta \cdot n + 1), \quad (14)$$

and it does not depend on the previous gains. Therefore, in this case, it is clear that non-increasing gains can always attain the optimum of REGS and, at the same time, maximize the SE, as discussed in Sec. 2.2.

While non-increasing gains already provide reductions in energy consumption when using an OJDR, the subtle differences between problems EGS and REGS show that optimum gain selection for quantum communication networks is an important nontrivial aspect of quantum network design by itself.

2.4 Minimizing amplifier energy consumption: Numerical Results

Using α , L and the number K of segments as an input, we can now optimize the gain profile to solve problems 12 and 13 for concrete cases that are matched to the technical reality of optical fiber networks. In Figure 2 we display an overview of our findings when the system is operating a single channel with typical values of wavelength $\lambda = 1550$ nm, maximum input power $w = 0.1$ mW and attenuation coefficient $\alpha = 0.05$ km⁻¹. Similar results for different system parameters are summarized in Figure 3. An overview including more amplifiers and longer links is presented in Figure 4. The algorithm employed to calculating the energy savings is explained in Methods 5.3. Details regarding our choice of photon number per pulse are in Section 2.4.1.

Figure 2 shows that the use of OJDR technology allows for energy savings for all combinations of distance and number of amplifiers. We plot the percentage of energy spent by OJDR with respect to a fully-amplified link with OSSR, i.e., $E_{\text{egs,regs}}/E_{\text{sh}}$, as a function of the link length and the number of segments. Furthermore, we consider two operational criteria to evaluate the practical relevance of our findings, aimed at identifying when the classical transmission system benefits the most from amplification:

- (i) the Shannon SE enhancement attainable by full amplification compared to no amplification, i.e. the ratio $AE := S_{\text{sh}}^{\text{op}}(n)/S_{\text{sh}}(n, \{1\}_{i=1}^K)$ (constant along white lines in Figure 2);
- (ii) the Shannon SE achievable by full amplification $S_{\text{sh}}^{\text{op}}(n)$ (constant along black lines in Figure 2).

The record savings for a photon number of $n = 10^7$ along the white line where $AE = 2$ in Figure 2 amount to 55% and occur at a total link length of 225 km when the link is using one amplifier placed at a distance of 112.5 km from the sender. For this configuration, the SE reached with amplification is ≈ 14.1 bits/s/Hz and that without amplification is ≈ 7.0 bits/s/Hz when an OSSR is used and ≈ 8.5 bits/s/Hz when an OJDR is employed.

A collective study over different photon numbers per pulse $n = 10^2, 10^3, \dots, 10^9$, modelling input energies 0.001 mW, \dots , 10 W at the sender is depicted in Figure 3.

We note further that even larger energy savings appear in situations of lesser practical relevance for commercial optical-fiber networks, which have been previously studied in terms of SE [6, 7, 11] and in terms of energy-efficiency in the limit where OSSR approximates OJDR [10] (bottom-right

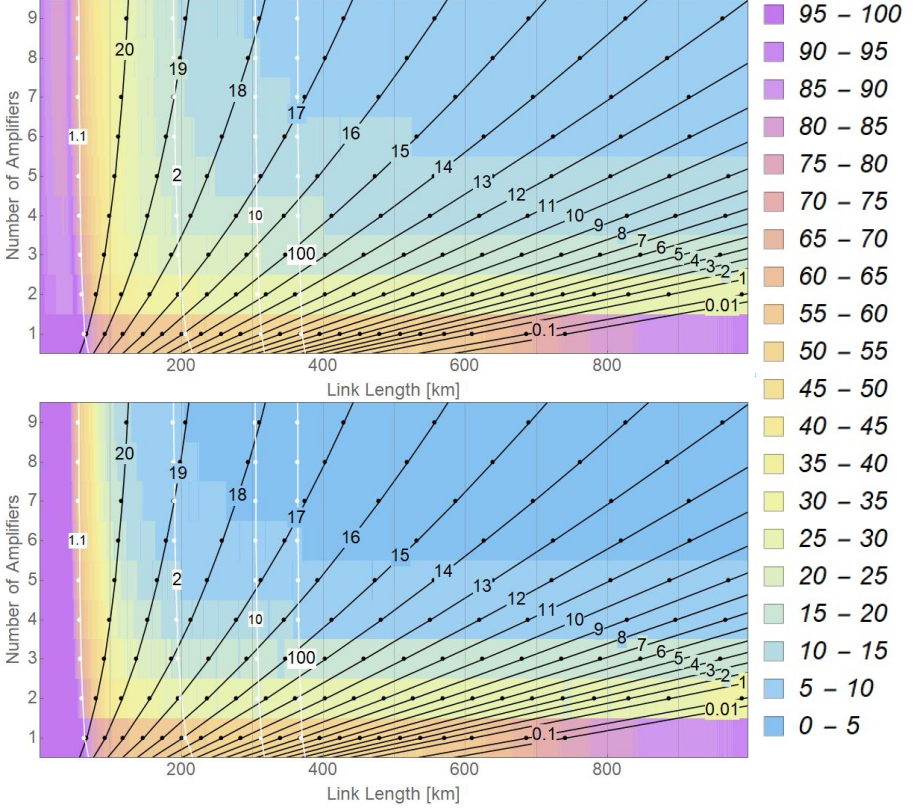


Fig. 2 Displayed is the percentage of energy used by the in-line amplifiers of links operating an OJDR relative to the same link with OSSR, as a function of link length and number of amplifiers. The top (bottom) image shows energy savings calculated according to problem EGS (REGS). The photon number is set to $n = 10^7$, corresponding to a maximum signal power of 100mW. SE is constant along black lines. The gain AE achieved from the use of amplifiers is constant along white lines. Interesting areas are those to the right of the second white line (at least two-fold gain from amplification) and to the left of the eighth black line counted from the right (indicating a spectral efficiency of at least 6 bits/s/Hz).

and upper-left regions of Figure 2). Indeed, at least 95% of the energy can be saved by the OJDR in the regimes of long distance, though with extremely low achievable SE, and short distance, though with extremely low enhancement compared to the unamplified case.

Finally, the qualitative difference between our approximate solutions to problems EGS and REGS are shown in Figure 2 to be quite small (on average over the data presented in Figure 2 it amounts to $\approx 5\%$, with a maximum difference in the energy savings of $\approx 23\%$), implying that a simple decreasing-gain profile already provides near-optimal energy savings for a large number of configurations.

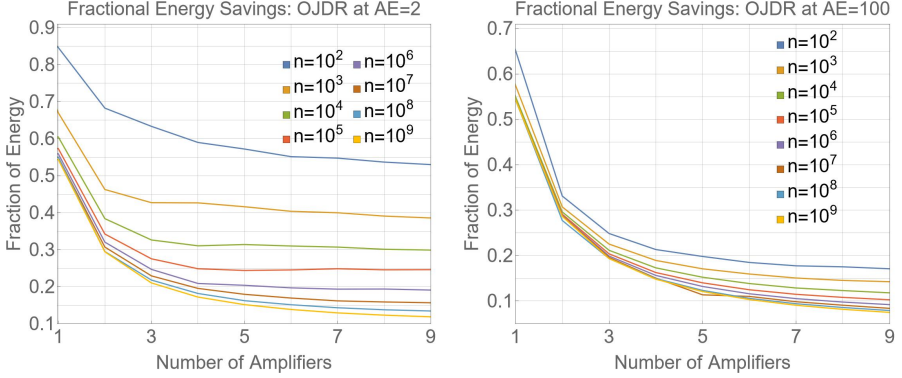


Fig. 3 Displayed are the energy savings vs. the number of amplifiers for different values of the photon number n , at those points where $AE = 2$ (left) and $AE = 100$ (right). For the particular value of $n = 10^7$, these are the points along the white lines labelled with 2 and 100 in Figure 2.

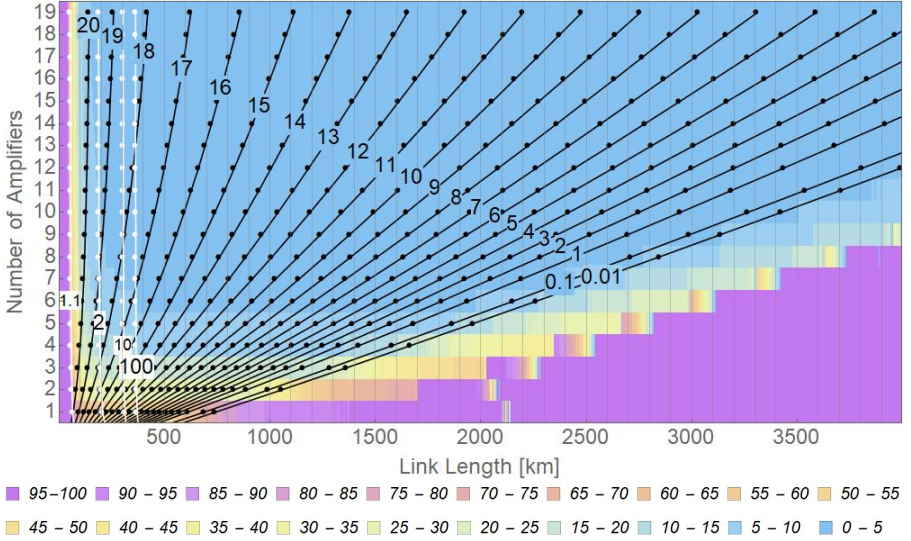


Fig. 4 Displayed is the percentage of energy used by the in-line amplifiers of links operating an OJDR relative to the same link with OSSR, as a function of link length and number of amplifiers. The photon number is set to $n = 10^7$, SE is constant along black lines. The gain AE achieved from the use of amplifiers is constant along white lines.

2.4.1 Parameter Choices

The photon numbers per pulse used to calculate the Shannon and Holevo SE (4.5) in this work are motivated from calculations targeted at fitting the model parameters to the real-world setting.

We consider a system operating a single channel at the prototypical wavelength $\lambda = 1550$ nm of the C-band, and a laser output power of $w = 0.1$ mWatts. The baud-rate, i.e. the number of pulses per second, is fixed to

$b = 80$ Giga pulses/s (equivalent to 80 Gbaud), a number which is in line with currently used numbers for fiber-optical transmission systems [38]. The energy per photon can be calculated using Planck's constant as

$$e_p = \frac{h \cdot c}{1550 \text{ nm}}, \quad (15)$$

where c is the speed of light. It satisfies $e_p \approx 0.1$ AttJ. To be in a commercially interesting range of photon numbers we study situations where the laser output power w in Watt is between $0.1 \mu\text{W}$ and 10 mW . The laser output power fixes the number of photons per pulse via

$$w = e_p \cdot n \cdot b. \quad (16)$$

Correspondingly, we take a rounded value of $n = 10^7$ to study transmission at 100 mW . Our model predicts a large potential for energy savings resulting from the use of OJDRs. To make sure this prediction does not just depend on our choice of parameters, we study also systems with photon numbers $n \cdot 10^{-3}$, $n \cdot 10^{-2}$, $n \cdot 10^{-1}$, $n \cdot 10^1$ and $n \cdot 10^2$.

For the cases where the photon number per pulse equals n , $10n$ and $100n$, non-amplified transmission over 80 km and with $\alpha = 0.05 \text{ 1/km}$ our model predicts Shannon SEs of 17 bits/s/Hz , 21 bits/s/Hz and 24 bits/s/Hz . The data transmission rates corresponding to these parameter choices are then given by multiplying the Shannon SEs with the baudrate, and evaluate to 1.4 Tbit/s , 1.7 Tbit/s and 1.9 Tbit/s . A comparison with the literature reveals these numbers to be roughly in the range of the possible, yet unrealistically high. Since our model ignores any noise that is not resulting from optical amplification, and also disregards any effects arising from the nonlinear interaction of the pulses with the fiber, these deviations seem reasonable.

3 Communication in the Quantum Limit

We have so far quantified the possibility of energy savings in amplifiers based on the use of the OJDR, with a main focus on the current system parameters.

To point out the timeliness and usefulness of quantum receiver technology also with regards to future system architectures, we consider here in addition the limit of high baud rates.

The key idea of this section follows the reasoning of operating a communication system in a parameter regime which is chosen in an attempt to harness the superior performance of quantum data transmission techniques. When a power constraint is imposed on a communication link with a large enough spectral bandwidth, high-baud-rate transmission systems naturally operate on a low photon number per pulse. The technological feasibility of such a system must then be answered based on the imposed bandwidth limitations and the available processing speed of the receiver in conjunction with the expected added value arising from the novel system design.

The interesting observation one can make based on formulas (4) and (5) is that for a fixed maximum allowed number N of photons per second, the number of photons per pulse (at the transmitter) satisfies $n = N/b$ where b is the number of pulses per second (also called baud-rate). At a given attenuation τ and noise level ν per pulse, the number of bits per second that can be transmitted using an OSSR saturates for high baud-rates:

$$\lim_{b \rightarrow \infty} \log \left(1 + \frac{\tau \cdot \frac{N}{b}}{1 + \nu} \right) \cdot b = \frac{N \cdot \tau}{(1 + \nu) \ln(2)} \leq \frac{N \cdot \tau}{\ln(2)}, \quad (17)$$

whereas the corresponding quantity for an OJDR diverges at zero thermal noise:

$$\lim_{b \rightarrow \infty} \left(g \left(\tau \cdot \frac{N}{b} + \nu \right) - g(\nu) \right) \cdot b = N \cdot \tau \cdot \log \left(1 + \frac{1}{\nu} \right) \quad (18)$$

Thus since the spectral bandwidth scales with baud rate b , settings of low thermal noise and high spectral bandwidth will allow the OJDR to outperform the OSSR by any arbitrary factor.

If also the thermal noise per second stays constant while the baud-rate increases, this noise per pulse equals ν/b . In such a scenario, the limiting expression for the OJDR is obtained by noting that for any $x, y > 0$ we have

$$g\left(\frac{x}{b}\right) \cdot b = x \cdot \log\left(1 + \frac{b}{x}\right) + b \cdot \log\left(1 + \frac{x}{b}\right). \quad (19)$$

Using the limiting expressions $\lim_{b \rightarrow \infty} b \cdot \log(1 + x/b) = x/\ln(2)$ and $\lim_{b \rightarrow \infty} \log(1 + \frac{b}{x}) - \log(1 + \frac{b}{y}) = \log(\frac{y}{x})$ we know that for each choice of (N, τ, ν) there exists a sequence $(\epsilon_b)_{b \in \mathbb{R}}$ and a constant $\epsilon = \epsilon(N, \tau, \nu)$ such that $\epsilon_b \rightarrow \epsilon$ and

$$\left(g \left(\tau \cdot \frac{N}{b} + \frac{\nu}{b} \right) - g\left(\frac{\nu}{b}\right) \right) \cdot b = \tau \cdot N \cdot \log\left(\frac{b}{\tau \cdot N + \nu}\right) + \epsilon_b. \quad (20)$$

Thus for every choice of N, τ and ν the dependence of the channel capacity on the baud-rate is effectively logarithmic and grows unbounded as $\tau \cdot N \cdot \log(\frac{b}{\tau \cdot N + \nu})$ when using an OJDR. In sharp contrast, the capacity of the same channel using an OSSR is limited by $\frac{\tau \cdot N}{\ln(2)}$. As the latter bound applies in particular also when amplifiers are used, the use of high baud-rates provides an opportunity for non-amplified networks. This new possibility is of high relevance for future integrated classical- and quantum networks, which might need to transmit classical messages on the same shared medium as quantum services. For transmission and maintenance of entangled states, noise is a challenging problem. Thus for integrated networks, where noise needs to be avoided at all costs, it is important to observe that there exist quantum data transmission methods which avoid the noise induced by amplification in data transmission, so that the resulting noiseless networks become an ideal starting point for quantum network development.

To investigate the current hypothetical advantage of quantum communication methods in high baud-rate transmission, it is insightful to consider parameters matched to existing networks. Transmission with center wavelength at 157.5nm would allow for a maximum baud rate in the order of $b \approx 18000$ GigaBaud. At this baud rate, the number of bits per second for transmission over a cable of length $L = 185$ km at 1 mW is ≈ 1 TeraBit/s with an OSSR and ≈ 4.3 TeraBit/s with an OJDR - more than a 4-fold increase in data transmission rate, which is mainly limited by the carrier frequency and the spectral bandwidth limitations imposed by the physical properties of optical fiber in the C-band, plus potentially the processing speed of electronic gates in the receiver. For both problems, solutions are in principle possible:

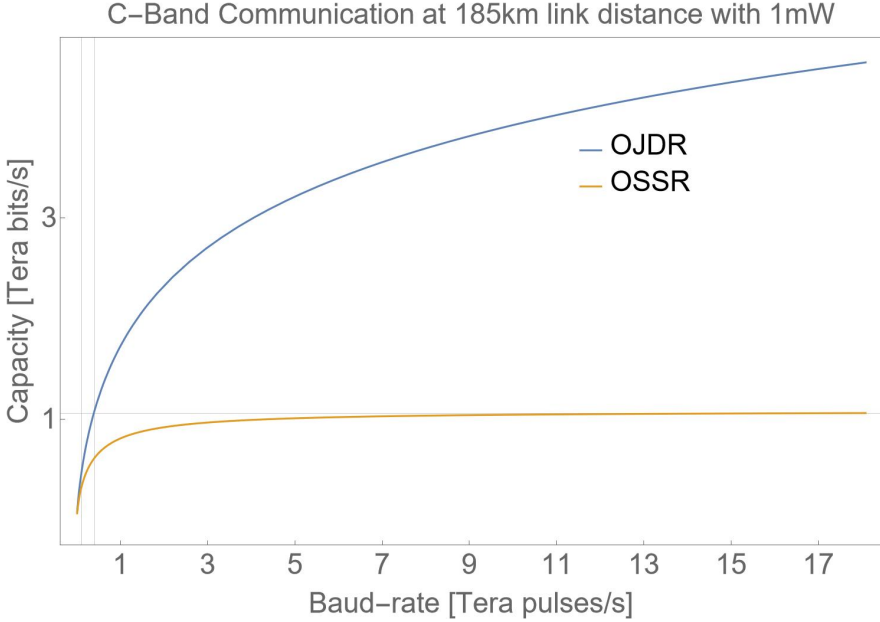


Fig. 5 Displayed is the growth of capacity in bits per second as a function of baud-rate at a distance of 185km with 1mW transmit power at the sender and attenuation coefficient of $\alpha = 0.05 \text{ km}^{-1}$. The vertical line at baud-rate $b = 0.1 \cdot 10^{12}$ shows where a current commercial system operates. The vertical line at $0.44 \cdot 10^{12}$ marks the beginning of the quantum limit.

hollow-core fibers can be better tailored to the transmission of ultra-short pulses [24, 25, 39], and optical processing as a physical-layer technique can utilize the principles of quantum-mechanical detection based on newly developed integrated optics techniques.

Spreading the signal energy for data transmission over a wide spectral range might in addition open up a way for co-existence of data transmission with other services of future quantum networks. Our analysis thus suggests an exciting new venue for quantum communication network development.

Finally we observe that, though the realization of a full-fledged OJDR is still an open problem, the Hadamard receiver [8, 9, 18, 23], realizable with integrated photonics, offers the opportunity to observe the high-baud-rate advantage enabled by a quantum receiver in a realistic setting. In the above setting of communicating in the C-band over 185 km at 1 mW, Hadamard codes with orders 4, 8, 16, 32 would offer respective transmission rates of 1.3799 Tbit/s, 1.911 91 Tbit/s, 2.189 87 Tbit/s, 2.0744 Tbit/s. These rates can be calculated in the zero-noise case as

$$\frac{b}{k} \left(1 - \exp \left(-\frac{k\tau n}{b} \right) \right) \log k, \quad (21)$$

using for example Ref. [8].

4 Discussion

We have shown that the introduction of a quantum detection method, the OJDR, can reduce the energy cost of a fiber-optical communication line by up to $\approx 55\%$, in a practically relevant parameter regime where optical amplifiers enable to maintain a large communication rate.

This determines, for the first time to our knowledge, a striking energy advantage of quantum vs. classical detection methods for the transmission of classical information on optical fiber. Our results highlight the relevance of QIP in communication beyond the traditional settings of secure-communication and entanglement-transmission, opening up a third research direction with potentially closer-term applications, which is fully compliant with the vision of all-optical networking [40].

It is well-known that the performance of quantum receivers approaches that of their classical counterparts under high noise. Resulting from this fact is a perception that quantum receiver technology might not be relevant in practical applications, where noise cannot be avoided. Our approach inverts the argument: by reducing the amplifier gains along the line we reduce the noise resulting from spontaneous emission, thereby moving towards the regime where the quantum receiver is superior while at the same time reducing the energy consumption of the amplifiers.

Along this line of argument, we have shown that even a complete removal of amplifiers is possible, given enough spectral bandwidth supporting high baud-rates. We have described the respective scaling laws of the data transmission rates with the baud-rate for both OJDR and OSSR technology.

We stress that, although our analysis can be refined by employing more complex models of energy consumption, including non-linearities and the energy transfer towards the amplifiers, these effects can only increase energy consumption and hence provide further arguments in favour of the OJDR. Our results renew the urgency of devising an explicit optical receiver design that can approximate the OJDR at all signal energies and set the stage for

a redesign of established data transmission technology based on a use of quantum-mechanical principles.

In what follows, we list implications of our results which are relevant to other research domains in networking. Namely, OJDR technology can:

1) provide advantages already today: these come in terms of energy savings at amplifiers.

2) increase the length of non-amplified links: If new types of optical fiber with more spectral bandwidth were deployed, the observed initial savings could eventually translate into a complete removal of the amplifiers, without any sacrifice on the data rates.

3) lay the ground for quantum network development: A removal of amplifiers decreases the overall noise in the channel, and we can expect this to imply an increase of the quantum-data-transmission capacity. For example, consider the most basic instance of our communication line (Fig.1) with $K = 2$ optical-fiber links of loss η , separated by a quantum-limited amplifier of gain G . The overall channel, determined by (3), can be described as a thermal-attenuator bosonic channel with attenuation coefficient $G\tau^2$ and extra-noise coefficient $\frac{\tau(\tau+2)(G-1)}{2(1-G\tau^2)}$, in the notation of [41, Eq. (11)]. Both the upper and lower bounds [41, Eqs. (18,40)] appear to be decreasing as a function of the gain and hence one can expect that quantum communication benefits from the complete removal of amplifiers along the line⁴.

4) simplify network deployment and maintenance: The use of this technology in conjunction with high baud-rates offers a possibility to simplify deployment and operation of data networks that can be operated without amplifiers.

5) offer a way to evade noise induced by the Kerr effect: A consequence of our work is the emergence of transmission in the quantum limit as a new design option for fiber-optic networks. For such networks, the non-linear Shannon limit resulting among others from the Kerr effect imposes severe practical boundary conditions [45]. Optimization under these boundary conditions is an active research field [46]. The Kerr effect itself induces a specific type of noise to the system which depends on the signal energy [47] and thus eventually prevents a growth of the system capacity with the signal energy. Our approach does instead advertise communication in a low-energy regime where the Kerr effect has little impact, and where the capacity loss incurred from the lower energy is compensated for by high baud-rates. This approach is in line with the historic trend of pushing baud-rates to higher and even higher numbers, which is documented e.g. in [48].

The following is an important limitation in our analysis: We point out that our analysis rests on the established formulas for Shannon- [30] and

⁴The lower bound was first found in [42]. Better upper bounds at the considered noise and attenuation levels have been obtained in [43]. Obviously, the lack of an exact formula makes the decrease of the quantum capacity as a function of the gain a well-motivated conjecture, rather than a certainty. Furthermore, a more careful analysis of the above statement should rely on the study of the joint capacity region for classical and quantum communication [44].

Holevo [31] capacity, which take into account only attenuation and thermal noise. Any further effects arising from a use of ultra-short pulses are beyond the scope of our analysis. Thus our work justifies a more in-depth analysis of transmission media when operated in the quantum limit, which we define as the baud-rate at which the data transmission capacity of the link operated with an OJDR exceeds the upper bound imposed on that same link when operated with an OSSR.

In summary, our results mark the importance of QIP in terms of energy-efficiency, which is a metric of growing impact for optical network engineering. They vindicate the central role of quantum detection in optical communication technologies, and motivate a re-examination of quantum advantage beyond its traditional meaning in computation, metrology and communication.

5 Methods

5.1 Shannon and Holevo SEGS

For a given segment i in the transmission line, let us define the cumulative attenuation and noise coefficients of the future segments as

$$\tau_{>i} := \eta^{K-i} \prod_{j=i+1}^K G_j, \quad \nu_{>i} := \sum_{j=i+1}^K (G_j - 1) \cdot \tau_{>j}. \quad (22)$$

In terms of these, the total attenuation and noise coefficients can then be written as

$$\tau = \tau_{>i} \cdot \tau_i, \quad \nu = \tau_{>i} \cdot \nu_i + \nu_{>i}. \quad (23)$$

5.1.1 Non-increasing gains maximize the SE

We start by proving that increasing gains are sub-optimal for information transmission on our multi-span amplified optical-fiber transmission line. Consider a channel where two consecutive gains are in increasing order, i.e., $G_i < G_{i+1}$. Then, the channel obtained by switching such gains, i.e., $G'_i := G_{i+1} > G'_{i+1} := G_i$, is characterized by the same attenuation coefficient $\tau' = \tau$, since it contains the product of all the gains, and a smaller noise coefficient $\nu' < \nu$. Indeed, we can write the new noise coefficient as

$$\begin{aligned} \nu' &= \tau'_{>i} \cdot \nu'_i + \nu'_{>i} \\ &= \tau_{>i+1} \cdot G'_{i+1} \eta \cdot (G'_i \eta \cdot \nu_{i-1} + G'_i - 1) + (G'_{i+1} - 1) \cdot \tau_{>i+1} + \nu_{>i+1}, \end{aligned} \quad (24)$$

where we used the fact that all gains at segments different from $i, i+1$ remained unchanged. Using the same decomposition for ν , and taking into account the

definition of G' , we can write the noise-difference as

$$\begin{aligned}\nu - \nu' &= \tau_{>i+1} \cdot [-\eta \cdot (G_{i+1} - G_i) + G_{i+1} - G_i] \\ &= \tau_{>i+1} \cdot (G_{i+1} - G_i) \cdot (1 - \eta) > 0.\end{aligned}\quad (25)$$

Hence, the channel with increasing gains can be obtained from the channel with decreasing gains by composition with a Gaussian additive-noise channel of noise parameter $\nu - \nu'$. By the data-processing inequality applied to the classical or quantum mutual information, this implies that the channel with decreasing gains can transfer more information, independently of the communication method employed [49].

5.1.2 Shannon SEGS

Let us now prove that the Shannon SE is monotonically increasing as a function of the gains $G_{i < K}$. First observe that S_{sh} is an increasing function of the signal-to-noise ratio $\text{SNR} := \tau \cdot n / (1 + \nu)$. Then express the derivatives of the attenuation and noise coefficients with respect to gain G_i as follows:

$$\frac{\partial \tau}{\partial G_i} = \tau_{>i} \cdot \eta = \frac{\tau}{G_i}, \quad \frac{\partial \nu}{\partial G_i} = \tau_{>i} \cdot (\eta \cdot \nu_{i-1} + 1) = \frac{\nu - \nu_{>i} + \tau_{>i}}{G_i}, \quad (26)$$

where we have employed (23). Substituting these expressions into the derivative of the SNR we finally obtain

$$\begin{aligned}\frac{\partial \text{SNR}}{\partial G_i} &= \frac{\text{SNR}}{G_i} - \frac{\text{SNR}}{1 + \nu} \cdot \frac{\nu - \nu_{>i} + \tau_{>i}}{G_i} \\ &= \frac{\text{SNR}}{G_i} \cdot \frac{1 - \tau_{>i} + \nu_{>i}}{1 + \nu} \geq 0,\end{aligned}\quad (27)$$

since $\tau_i \leq 1$ by (6). In particular, equality is attained only for $i = K$, while for $i < K$ the Shannon SE is strictly increasing and hence the optimal gain profile is that with $G_{i < K} = G_{\text{max}}$.

5.1.3 Holevo SEGS

The results are quite different for the Holevo SE. Considering that $g'(x) = \log(1 + 1/x)$, we can write

$$\begin{aligned} \frac{\partial S_{\text{ho}}}{\partial G_i} &= \left(\frac{\tau}{G_i} \cdot n + \frac{\nu - \nu_{>i} + \tau_{>i}}{G_i} \right) \log \left(1 + \frac{1}{\tau \bar{n} + \nu} \right) \\ &\quad - \left(\frac{\nu - \nu_{>i} + \tau_{>i}}{G_i} \right) \log \left(1 + \frac{1}{\nu} \right) \\ &= \frac{1}{G_i} \log \frac{f_{\beta_i}(\tau \cdot n + \nu)}{f_{\beta_i}(\nu)}, \end{aligned} \quad (28)$$

where $f_{\beta}(x) := (1 + \frac{1}{x})^{x+\beta}$ and $\beta_i = \tau_{>i} - \nu_{>i} \leq 1$. Hence, the sign of (28) is determined by the behaviour of f for different values of β . It can be checked that $f_{\beta}(x)$ is a monotonically increasing function of x for $\beta \leq 0$, while it is monotonically decreasing for $\beta \geq 1/2$; instead, for $0 < \beta < \frac{1}{2}$ it has a global minimum at intermediate values of x , whose position moves from 0 to ∞ as β increases. We conclude that, as a function of G_i , the Holevo SE can be found in three distinct regimes:

- (i) no-amplification regime: in this case it holds $\beta_i \geq 1/2$, hence (28) is strictly negative for all $n > 0$, independently of the other gains, and S_{ho} is maximum at $G_i = 1$;
- (ii) maximum-gain regime: in this case it holds $\beta_i \leq 0$, hence (28) is strictly positive for all $n > 0$, independently of the other gains, and S_{ho} is maximum at the maximum allowed value of gain $G_i = G_{\text{max}}$;
- (iii) intermediate regime: in this case it holds $0 < \beta_i < 1/2$ and the sign of (28) must be determined on a case-to-case basis depending on τ, ν, n and the optimization cannot be carried out independently of the other gains. Still, it can happen that the optimal gain value is minimum. Indeed, calling x_{β_i} the minimum of $f_{\beta_i}(x)$, suppose that all the gains previous to G_i are at their maximum value and $\tau \cdot n + \nu < x_{\beta_i}$; then (28) is strictly negative for that particular choice of gains but also for any smaller values of those gains; since decreasing any gain will decrease both τ and ν , preserving the previous inequality. Hence it will be possible to set $G_i = 1$ also in this case.

Furthermore, another property that might be helpful in the optimization is that β_i is a non-decreasing sequence, since

$$\beta_i = \tau_{>i} - (G_{i+1} - 1) \cdot \tau_{>i+1} - \nu_{>i+1} \quad (29)$$

$$= \tau_{>i} \left(1 - \frac{1}{\eta} \right) + \beta_{>i+1}, \quad (30)$$

where we have written explicitly the first term in the decomposition of $\nu_{>i}$ and recalled that $\tau_{>i} = \eta \cdot G_i \cdot \tau_{i-1}$.

In conclusion, the analytical optimization of S_{ho} seems difficult. Still, the above-described properties allow very easily to identify parameter regimes that ensure that at least one gain is minimum, e.g., the condition $1/2 \leq \beta_{K-1} = \eta$ implies $G_{K-1}^{\text{op}} = 1$, proving that $S_{\text{ho}}^{\text{op}} > S_{\text{ho}}(n, \{G_{i < K} = G_{\text{max}}, G_K = 1\})$ in general.

The nontrivial dependence of Holevo SE on the gain profile can be illustrated in the situation of continuous amplification:

5.2 Energy savings with continuous amplification

Here we show that energy gains can be obtained by using an OJDR vs. an OSSR even in the continuous-amplification limit. This is in contrast to the claim of Ref. [10], where the Holevo SE was studied only in the setting where an OJDR is comparable with an OSSR.

The optimal Shannon SE in the continuous-amplification limit can be determined by taking $K \rightarrow \infty$ in (9) and observing that $\eta \approx 1 - \alpha L/K$ in this limit:

$$S_{\text{sh}}^{\text{op}, \infty}(n) = \log \left(1 + \frac{e^{-\frac{\alpha L}{n+1}} \cdot n}{1 + \left(1 - e^{-\frac{\alpha L}{n+1}}\right) \cdot n} \right). \quad (31)$$

The corresponding energy cost is simply

$$E_{\text{sh}}^{\infty}(n) = \alpha L \cdot n. \quad (32)$$

In the case of the Holevo SE, we start by considering K finite segments, out of which only the first $\gamma \cdot K$ are amplified, for $\gamma \in [0, 1]$. This is a sub-optimal strategy for Holevo SEGS that still captures most of the relevant features of the problem and that can actually be optimal in some cases, based on the analysis of Methods 5.1.3. The corresponding attenuation and noise coefficients can be written as

$$\tau_K(\gamma) := e^{-\alpha L} \cdot \left(\frac{1+n}{1+\eta n} \right)^{\gamma K}, \quad \nu_K(\gamma) = \left(e^{-\alpha L(1-\gamma)} - \tau_K(\gamma) \right) \cdot n, \quad (33)$$

and, in the limit $K \rightarrow \infty$ with γ fixed approach

$$\tau_{\infty}(\gamma) = \exp \left[-\alpha L \left(1 - \frac{\gamma \cdot n}{1+n} \right) \right], \quad \nu_{\infty}(\gamma) = \left(e^{-\alpha L(1-\gamma)} - \tau_{\infty}(\gamma) \right) \cdot n. \quad (34)$$

The corresponding SE and energy cost are

$$S_{\text{ho}}^{\infty}(n, \gamma) = g \left(e^{-\alpha L(1-\gamma)} \cdot n \right) - g(\nu_{\infty}(\gamma)) \quad (35)$$

$$E_{\text{ho}}^{\infty}(n, \gamma) = \alpha L \gamma \cdot n. \quad (36)$$

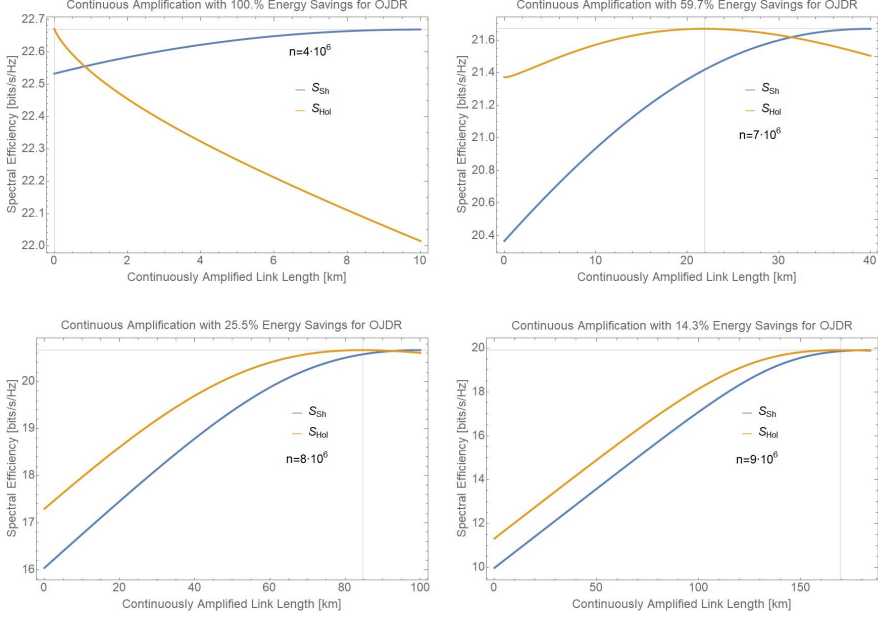


Fig. 6 Spectral efficiency of communication links with $L = 10$ km, 40 km, 100 km, 184 km (counting top down and from left to right) and $\alpha = 0.05\text{km}^{-1}$. The x axis denotes the length L_1 of the initial segment that is fully amplified. As expected, the Shannon spectral efficiency is monotone in L_1 . However, the spectral efficiency when using an OJDR is at the same value as the one when using an SSR at lengths $L_1 < L$ in all depicted scenarios. Moreover, the power constraint on the link can be reduced when OJDR is used so that energy savings can be harvested.

It is now possible to define an optimization problem similar to EGS for this on-off strategy:

$$\begin{aligned}
 E_{\text{oo}} &:= \underset{n, \gamma}{\text{minimize}} \quad E_{\text{ho}}^{\infty}(n, \gamma) \\
 &\text{subject to : } 0 \leq n \leq n_0, 1 \leq \gamma \leq 1 \\
 &\quad S_{\text{ho}}^{\infty}(n, \gamma) \geq S_{\text{sh}}^{\text{op}, \infty}(n_0).
 \end{aligned} \tag{37}$$

Here, both the maximum power at any point on the segment can be optimized and the length of the initial, amplified segment. Setting e.g. the power constraint for communication with the OSSR to $n_0 = 10^7$, a multitude of different energy savings can be realized, which highlight the nontrivial dependency of the communication link on the gain profile even in the limit of continuous amplification. Note that all situations depicted in Figure 6 have a value of $AE < 2$, except the one with $L = 184$ km where $AE \approx 2$ holds.

5.3 Algorithm

Here we describe the algorithm we employed to solve the optimization problems EGS and REGS.

For both these problems, since the feasible region is closed and bounded and the objective function continuous, the Weierstrass theorem guarantees the existence of a global optimum. However, the function S_{ho} is in general neither convex nor concave.

We applied several numerical methods to find approximate solutions to problems 12 and 13. The most efficient one turned out to be a gradient-based method that we describe in the following. The general approach is identical for both EGS and REGS and also for the optimization of energy consumption when homodyne detection is employed.

Starting from maximum gains, the method iterates between optimizing the energy consumption E (or E' for REGS) following the gradient ∇E (or $\nabla E'$ for REGS), and then optimizing energy consumption along a surface where S_{ho} is constant. Searching the solutions to REGS is particularly fast since $\nabla E'$ is constant.

Assuming that $G_K = 1$ is obeyed throughout so that it does not need to be listed as a variable, the two sub-routines are to follow the gradient of E with decreasing speed for several steps as described in Algorithm 1, and to follow along a surface where S_{ho} is constant as described in Algorithm 2.

Algorithm 1 energyGradient

Require: G_1, \dots, G_{K-1} , a , n , SE

```

1:  $s = 1$ 
2:  $\text{stepSize} \leftarrow (G_{\max} - 1)/2^{-s}$ 
3: while  $s < a$  do
4:    $x \leftarrow \|\nabla E\|^{-1} \cdot \nabla E$ 
5:    $(\hat{G}_1, \dots, \hat{G}_{K-1}) \leftarrow (G_1 - x_1 \cdot \text{stepSize}, \dots, G_{K-1} - x_{K-1} \cdot \text{stepSize})$ 
6:   if  $S_{\text{ho}}(n, \{\hat{G}_i^k\}_{i=1}^K) > SE$  and  $G_{\max} \geq \hat{G}_i \geq 1 \forall i \in \{1, \dots, K-1\}$  then
7:      $(G_1, \dots, G_{K-1}) \leftarrow (\hat{G}_1, \dots, \hat{G}_{K-1})$ 
8:   else  $s \leftarrow s + 1$ 
9:      $\text{stepSize} \leftarrow (G_{\max} - 1)/2^{-s}$ 
10:  end if
11: end while
12: return  $G^K$ 
    
```

The complete Algorithm 3 iterates between the two methods for a few rounds.

The algorithm we developed to find approximate solutions for EGS is based on heuristic analysis and numerical study of the problem. From Methods 5.1 and Methods 5.2 it is clear that the EGS problem is highly nontrivial in general. Our goal is thus to exploit the fact that we typically have values of η such that $n \gg \eta^{-1}$. This results in the maximum gain obeying $G_{\max} \approx \eta^{-1}$. For such values of n and η we have observed that the determinant of the Hessian matrix of S_{ho} , $\det(HS_{\text{ho}})$, is negative in a region around the gain value $(1, \dots, 1)$, while being positive for most parameter choices - in particular at $(G_{\max}, \dots, G_{\max})$.

Algorithm 2 spectralSurface**Require:** G_1, \dots, G_{K-1} , a , n , SE

```

1:  $s = 1$ 
2:  $\text{stepSize} \leftarrow (G_{\max} - 1)/2^{-s}$ 
3: while  $s < a$  do
4:    $eG \leftarrow \|\nabla E\|^{-1} \cdot \nabla E$ 
5:    $sG \leftarrow \|\nabla S_{\text{ho}}\|^{-1} \cdot \nabla S_{\text{ho}}$ 
6:    $x = eG - \langle sG, eG \rangle \cdot sG$ 
7:    $(\hat{G}_1, \dots, \hat{G}_{K-1}) \leftarrow (G_1 - x_1 \cdot \text{stepSize}, \dots, G_{K-1} - x_{K-1} \cdot \text{stepSize})$ 
8:   if  $S_{\text{ho}}(n, \{\hat{G}_i^k\}_{i=1}^K) > SE$  and  $G_{\max} \geq \hat{G}_i \geq 1 \forall i \in \{1, \dots, K-1\}$  then
9:      $(G_1, \dots, G_{K-1}) \leftarrow (\hat{G}_1, \dots, \hat{G}_{K-1})$ 
10:  else  $s \leftarrow s + 1$ 
11:     $\text{stepSize} \leftarrow (G_{\max} - 1)/2^{-s}$ 
12:  end if
13: end while
14: return  $G^K$ 

```

Algorithm 3 Gradient-based Optimization**Require:** G_{\max} , a , n ,

```

1:  $(G_1, \dots, G_{K-1}) \leftarrow (G_{\max}, \dots, G_{\max})$ 
2:  $SE \leftarrow S_{\text{sh}}(n, G^K)$ 
3: while  $s < a$  do
4:    $G^K \leftarrow \text{energyGradient}(G^K, s, n, SE)$ 
5:    $G^K \leftarrow \text{spectralSurface}(G^K, s, n, SE)$ 
6: end while
7: return  $G^K$ 

```

This observation justifies using $(G_{\max}, \dots, G_{\max})$ as the starting point for the algorithm. Moreover, letting the algorithm initially avoid setting a gain to one will let it effectively operate in a region where $\det(HS_{\text{ho}})$ is positive, so that the algorithm acts as if optimizing over a convex region.

The approach of initially moving along the gradient ∇E of $E(\cdot)$ is thus a suitable approach. The entries of ∇E are calculated based on the partial derivatives

$$\partial_{G_i} E(G^K) = \eta(\tau_{i-1}n + \nu_{i-1}) + 1 + \sum_{k=i+1}^K (G_k - 1)\eta(\partial_{G_i}\tau_{k-1}n + \partial_{G_i}\nu_{k-1}), \quad (38)$$

with $G^K := \{G_i\}_{i=1}^K$. The derivative $\partial_{G_i}\tau_{k-1}$ equals $G_1 \dots G_{i-1} \cdot G_{i+1} \dots G_{k-1}\eta^{k-1}$. The derivatives $\partial_{G_i}\nu_{k-1}$ are calculated based on the matrix

$$M(G) := \begin{pmatrix} \eta \cdot G & G - 1 \\ 0 & 1 \end{pmatrix} \quad (39)$$

which, using the canonical basis vectors e_1, e_2 , lets us compute each ν_k as

$$\nu_k = \langle M(G_k) \cdot \dots \cdot M(G_1) e_2, e_1 \rangle. \quad (40)$$

Denoting with $D(G) := \partial_G M(G)$ the derivative of M at point G , the derivative of ν_k with respect to G_i is (if $i < k$)

$$\partial_{G_i} \nu_k(G^k) = \langle M(G_k) \dots M(G_{i+1}) \cdot D(G_i) \cdot M(G_{i-1}) \dots M(G_1) e_2, e_1 \rangle. \quad (41)$$

For the large values of n studied in this work the approximation $G_{\max} \approx \eta^{-1}$ holds. At the point $G^K = (\eta^{-1}, \dots, \eta^{-1}, 1)$ however we have (for $i < k$) the special situation that

$$M(\eta^{-1})^{i-1} = \begin{pmatrix} 1 & (i-1)(\eta^{-1} - 1) \\ 0 & 1 \end{pmatrix} \quad (42)$$

$$D(\eta^{-1}) M(\eta^{-1})^{i-1} = \begin{pmatrix} \eta & (i-1)(1-\eta) + 1 \\ 0 & 0 \end{pmatrix}. \quad (43)$$

Further it holds $M(\eta^{-1})^{k-i+1} D(\eta^{-1}) M(\eta^{-1})^{i-1} = D(\eta^{-1}) M(\eta^{-1})^{i-1}$, so that

$$\partial_{G_i} \nu_k(G^k) = i - (i-1)\eta, \quad (44)$$

$$\partial_{G_i} \tau_{k-1} n = \eta n, \quad (45)$$

$$\nu_{i-1} = (i-1)(\eta^{-1} - 1). \quad (46)$$

Thus since $\eta < 1$ we have $x := \frac{1}{\eta} - 1 > 0$ and can lower bound the components of the gradient ∇E as

$$\partial_{G_i} E(G^K) = \eta(n + (i-1)x) + 1 + \sum_{k=i+1}^K x \cdot \eta^2(n + 1 + i \cdot x) \quad (47)$$

$$\geq \eta \cdot n + 1. \quad (48)$$

Since K is at most 20 in all the situations we investigated, $n \gg x$ and $\eta \gg \eta^2$, the above lower bound is approximately tight within the limits of our heuristic analysis. A typical situation for two gains is presented in Figure 5.3. From above estimates we conclude the initial step of our optimization will typically avoid reducing one of the gains drastically, so that the algorithm effectively behaves as if optimizing over a convex region where $\det(HS_{\text{ho}}) > 0$.

Based on the available equations (28) for the derivatives of the Holevo SE, ∇S_{ho} is available as well.

5.4 Shannon performance with homodyne detection

In [35] it was shown that the best Gaussian receivers for communication on lossy bosonic channels (including the one studied in this paper) are heterodyne,

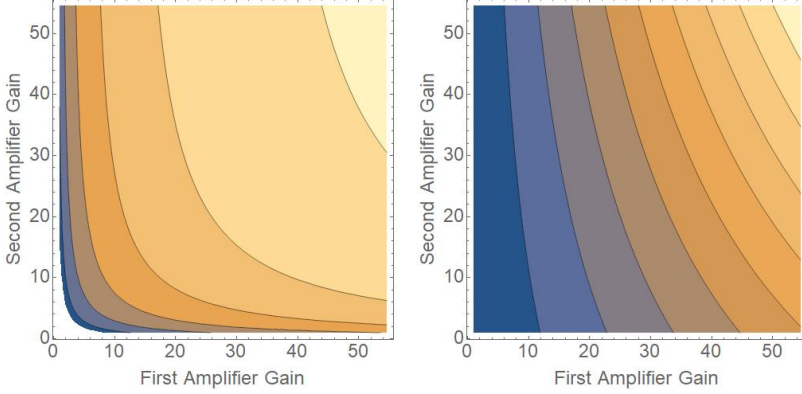


Fig. 7 Displayed is a contour plot of the Holevo SE (left) and of the energy consumption (right) for $n = 10^7$, $\alpha = 0.05$ and $L = 240$ km. The maximum gain in this case is ≈ 54.6 .

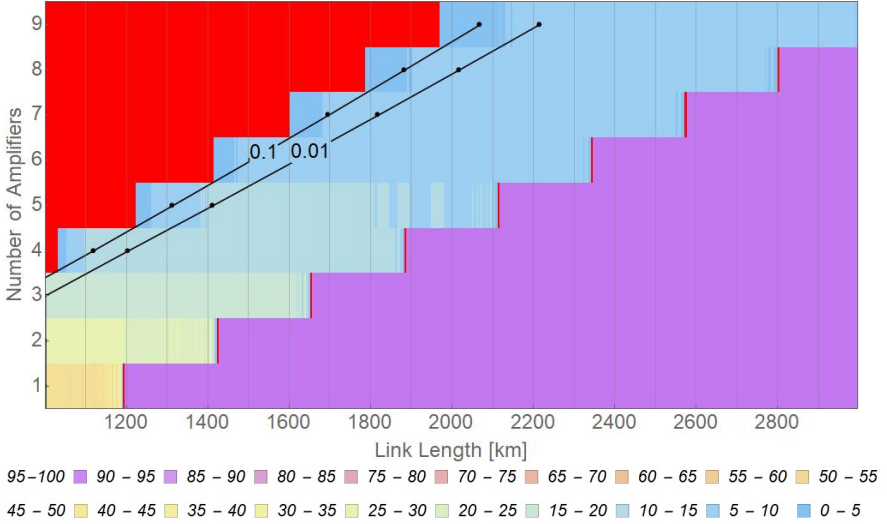


Fig. 8 Displayed are the energy savings achievable with homodyne OSSR over heterodyne OSSR. In the red region, the homodyne receiver is inferior to the heterodyne one. In the violet region, the savings are above 95%.

homodyne or a time-sharing between the two. The transition between the heterodyne-optimal and homodyne-optimal regimes takes place as the energy of the attenuated signal decreases, around $\tau \cdot n \approx 2$. Moreover, since the OSSR for Gaussian channels has been recently proved to be Gaussian [37], we conclude that the hetero/homodyne receiver coincides with the OSSR for our channel.

In the main text we focused on comparing the performance of the heterodyne receiver with the OJDR, observing a striking energy advantage of the latter. Here instead we briefly compare the performance of the homodyne

receiver with the OJDR. The Shannon SE attained by using the homodyne receiver is [35]

$$S_{\text{sh}}^{\text{hom}}(n) := \log \left(1 + \frac{4\tau \cdot n}{1 + 2\nu} \right). \quad (49)$$

For this quantity, the SEGs gain profile can in general be different from full amplification, similarly to the Holevo SE. Indeed, defining the signal-to-noise ratio as $\text{SNR}' := 4\tau \cdot n/(1 + 2\nu)$ and using the same notation as Methods 5.1, we have

$$\begin{aligned} \frac{\partial \text{SNR}'}{\partial G_i} &= \frac{\text{SNR}'}{G_i} - \frac{\text{SNR}'}{1 + 2\nu} \cdot 2 \cdot \frac{\nu - \nu_{>i} + \tau_{>i}}{G_i} \\ &= \frac{\text{SNR}'}{G_i} \cdot \frac{1 - 2\beta_i}{1 + \nu}. \end{aligned} \quad (50)$$

Since $\beta_i \leq 1$ for all i , this derivative can be negative and hence we can conclude that in general the homodyne SE will be maximized by non-maximum gains. In particular, if this holds in a region where the homodyne receiver can surpass the heterodyne receiver, we can expect the former to also offer an energy advantage with respect to the heterodyne receiver. For this reason, we also analyzed the EGS problem when using a homodyne receiver instead of the OJDR. The results, shown in Figure 5.4, confirm that the advantage of OJDR is much more pronounced, particularly in the practically relevant region identified in the main text. For example, in the same setting where the OJDR has record savings of 55%, the homodyne detector offers no savings at all - its SE is below 8 bits/s/Hz, while that of the fully amplified link with OSSR reach a value of above 14 bits/s/Hz.

Acknowledgments. Matteo Rosati gratefully acknowledges Marco Fanizza, for useful discussions of the results and for pointing out the use of data-processing to remove the last amplifier, as well as Andreas Winter, for useful discussions on the gap between Holevo and Shannon capacities. Janis Nötzel gratefully acknowledges stimulating discussions on the topic with Marcin Jarzyna and Konrad Banaszek during his visit at the CeNT.

This project has received funding from the DFG Emmy-Noether program under grant number NO 1129/2-1 (JN) and the European Union's Horizon 2020 research and innovation programme under the Marie Skłodowska-Curie grant agreement No 845255 (MR). Janis Nötzel further acknowledges the financial support by the Federal Ministry of Education and Research of Germany in the programme of "Souverän. Digital. Vernetzt.". Joint project 6G-life, project identification number: 16KISK002, and of the Munich Center for Quantum Science and Technology (MCQST). Both authors thank the participants of EACN 2022, and in particular Dan Kilper, for pointing out the interesting properties of hollow-core fiber.

Declarations. The authors declare no competing interests.

References

- [1] Bayvel, P., Maher, R., Xu, T., Liga, G., Shevchenko, N.A., Lavery, D., Alvarado, A., Killey, R.I.: Maximizing the optical network capacity. *Phil. Trans. R. Soc. A* **374**2014044020140440. <https://doi.org/10.1098/rsta.2014.0440>
- [2] Van Heddeghem, W., Lambert, S., Lannoo, B., Colle, D., Pickavet, M., Demeester, P.: Trends in worldwide ICT electricity consumption from 2007 to 2012. *Comput. Commun.* **50**, 64–76 (2014). <https://doi.org/10.1016/j.comcom.2014.02.008>
- [3] Kilper, D.C., Houman, R.: Energy challenges in optical access and aggregation networks. *Phil. Trans. R. Soc. A* **374**2014043520140435. <https://doi.org/10.1098/rsta.2014.0435>
- [4] Elshaari, A.W., Pernice, W., Srinivasan, K., Benson, O., Zwiller, V.: Hybrid integrated quantum photonic circuits. *Nat. Photonics* **14**(5), 285–298 (2020). <https://doi.org/10.1038/s41566-020-0609-x>
- [5] Wang, J., Sciarrino, F., Laing, A., Thompson, M.G.: Integrated photonic quantum technologies. *Nat. Photonics* **14**(5), 273–284 (2020). <https://doi.org/10.1038/s41566-019-0532-1>
- [6] Waseda, A., Takeoka, M., Sasaki, M., Fujiwara, M., Tanaka, H.: Quantum detection of wavelength-division-multiplexing optical coherent signals. *J. Opt. Soc. Am. B* **27**(2), 259 (2010). <https://doi.org/10.1364/JOSAB.27.000259>
- [7] Waseda, A., Sasaki, M., Takeoka, M., Fujiwara, M., Toyoshima, M., Assalini, A.: Numerical Evaluation of PPM for Deep-Space Links. *J. Opt. Commun. Netw.* **3**(6), 514 (2011). <https://doi.org/10.1364/JOCN.3.000514>
- [8] Guha, S.: Structured Optical Receivers to Attain Superadditive Capacity and the Holevo Limit. *Phys. Rev. Lett.* **106**(24), 240502 (2011) [arXiv:1101.1550](https://arxiv.org/abs/1101.1550). <https://doi.org/10.1103/PhysRevLett.106.240502>
- [9] Rosati, M., Mari, A., Giovannetti, V.: Multiphase Hadamard receivers for classical communication on lossy bosonic channels. *Phys. Rev. A* **94**(6), 062325 (2016). <https://doi.org/10.1103/PhysRevA.94.062325>
- [10] Antonelli, C., Mecozzi, A., Shtaif, M., Winzer, P.J.: Quantum Limits on the Energy Consumption of Optical Transmission Systems. *J. Light. Technol.* **32**(10), 1853–1860 (2014). <https://doi.org/10.1109/JLT.2014.2309721>

- [11] Jarzyna, M., García-Patrón, R., Banaszek, K.: Ultimate capacity limit of a multi-span link with phase-insensitive amplification. In: 45th Eur. Conf. Opt. Commun. (ECOC 2019), pp. 8–484. Institution of Engineering and Technology, ??? (2019). <https://doi.org/10.1049/cp.2019.0742>. <https://digital-library.theiet.org/content/conferences/10.1049/cp.2019.0742>
- [12] Tucker, R.S.: Green Optical Communications—Part I: Energy Limitations in Transport. *IEEE J. Sel. Top. Quantum Electron.* **17**(2), 245–260 (2011). <https://doi.org/10.1109/JSTQE.2010.2051216>
- [13] Tucker, R.S.: Green Optical Communications—Part II: Energy Limitations in Networks. *IEEE J. Sel. Top. Quantum Electron.* **17**(2), 261–274 (2011). <https://doi.org/10.1109/JSTQE.2010.2051217>
- [14] Pillai, B.S.G., Sedighi, B., Guan, K., Anthapadmanabhan, N.P., Shieh, W., Hinton, K.J., Tucker, R.S.: End-to-End Energy Modeling and Analysis of Long-Haul Coherent Transmission Systems. *J. Light. Technol.* **32**(18), 3093–3111 (2014). <https://doi.org/10.1109/JLT.2014.2331086>
- [15] Lundberg, L., Andrekson, P.A., Karlsson, M.: Power Consumption Analysis of Hybrid EDFA/Raman Amplifiers in Long-Haul Transmission Systems. *J. Light. Technol.* **35**(11), 2132–2142 (2017). <https://doi.org/10.1109/JLT.2017.2668768>
- [16] Schumacher, B., Westmoreland, M.D.: Sending classical information via noisy quantum channels. *Phys. Rev. A - At. Mol. Opt. Phys.* **56**(1), 131–138 (1997). <https://doi.org/10.1103/PhysRevA.56.131>
- [17] Hausladen, P., Jozsa, R., Schumacher, B., Westmoreland, M., Wootters, W.K.: Classical information capacity of a quantum channel. *Phys. Rev. A - At. Mol. Opt. Phys.* **54**(3), 1869–1876 (1996) [arXiv:0412133v3](https://arxiv.org/abs/0412133v3) [arXiv:quant-ph]. <https://doi.org/10.1103/PhysRevA.54.1869>
- [18] Guha, S., Wilde, M.M.: Polar coding to achieve the Holevo capacity of a pure-loss optical channel. In: 2012 IEEE Int. Symp. Inf. Theory Proc., pp. 546–550. IEEE, ??? (2012). <https://doi.org/10.1109/ISIT.2012.6284250>. <http://ieeexplore.ieee.org/document/6284250/>
- [19] Wilde, M.M., Guha, S.: Polar codes for classical-quantum channels. *IEEE Trans. Inf. Theory* **59**(2), 1175–1187 (2013) [arXiv:1109.2591](https://arxiv.org/abs/1109.2591). <https://doi.org/10.1109/TIT.2012.2218792>
- [20] Lloyd, S., Giovannetti, V., Maccone, L.: Sequential projective measurements for channel decoding. *Phys. Rev. Lett.* **106**(25), 250501 (2011) [arXiv:arXiv:1012.0106v1](https://arxiv.org/abs/1012.0106v1). <https://doi.org/10.1103/PhysRevLett.106.250501>

- [21] Giovannetti, V., Lloyd, S., Maccone, L.: Achieving the Holevo bound via sequential measurements. *Phys. Rev. A* **85**(1), 012302 (2012) [arXiv:arXiv:1012.0386v1](https://arxiv.org/abs/1012.0386v1). <https://doi.org/10.1103/PhysRevA.85.012302>
- [22] Rosati, M., Giovannetti, V.: Achieving the Holevo bound via a bisection decoding protocol. *J. Math. Phys.* **57**(6), 062204 (2015) [arXiv:1506.04999](https://arxiv.org/abs/1506.04999). <https://doi.org/10.1063/1.4953690>
- [23] Klimek, A., Jachura, M., Wasilewski, W., Banaszek, K.: Quantum memory receiver for superadditive communication using binary coherent states. *J. Mod. Opt.* **63**(20), 2074–2080 (2016) [arXiv:1512.06561](https://arxiv.org/abs/1512.06561). <https://doi.org/10.1080/09500340.2016.1173731>
- [24] Couny, F., Benabid, F., Roberts, P.J., Light, P.S., Raymer, M.G.: Generation and photonic guidance of multi-octave optical-frequency combs. *Science* **318**(5853), 1118–1121 (2007) <https://www.science.org/doi/pdf/10.1126/science.1149091>. <https://doi.org/10.1126/science.1149091>
- [25] Hayes, J.R., Sandoghchi, S.R., Bradley, T.D., Liu, Z., Slavík, R., Gouveia, M.A., Wheeler, N.V., Jasion, G., Chen, Y., Fokoua, E.N., Petrovich, M.N., Richardson, D.J., Poletti, F.: Antiresonant hollow core fiber with an octave spanning bandwidth for short haul data communications. *Journal of Lightwave Technology* **35**(3), 437–442 (2017). <https://doi.org/10.1109/JLT.2016.2638205>
- [26] Giovannetti, V., García-Patrón, R., Cerf, N.J., Holevo, A.S.: Ultimate classical communication rates of quantum optical channels. *Nat. Photonics* **8**(10), 796–800 (2014) [arXiv:1312.6225](https://arxiv.org/abs/1312.6225). <https://doi.org/10.1038/nphoton.2014.216>
- [27] Giovannetti, V., Holevo, A.S., García-Patrón, R.: A Solution of Gaussian Optimizer Conjecture for Quantum Channels. *Commun. Math. Phys.* **334**(3), 1553–1571 (2015). <https://doi.org/10.1007/s00220-014-2150-6>
- [28] Mari, A., Giovannetti, V., Holevo, A.S.: Quantum state majorization at the output of bosonic Gaussian channels. *Nat. Commun.* **5**(1), 3826 (2014). <https://doi.org/10.1038/ncomms4826>
- [29] Holevo, A.S.: Coding theorems for quantum communication channels. In: *IEEE Int. Symp. Inf. Theory - Proc.*, p. 84 (1998). <https://doi.org/10.1109/ISIT.1998.708669>
- [30] Shannon, C.E.: A Mathematical Theory of Communication. *Bell Syst. Tech. J.* **27**(4), 623–656 (1948). <https://doi.org/10.1002/j.1538-7305.1948.tb00917.x>

- [31] Holevo, A.S.: Bounds for the Quantity of Information Transmitted by a Quantum Communication Channel. *Probl. Inform. Transm.* **9**(3), 177–183 (1973)
- [32] Rosati, M., Mari, A., Giovannetti, V.: Capacity of coherent-state adaptive decoders with interferometry and single-mode detectors. *Phys. Rev. A* **96**(1), 012317 (2017) [arXiv:1703.05701](https://arxiv.org/abs/1703.05701). <https://doi.org/10.1103/PhysRevA.96.012317>
- [33] Rosati, M., De Palma, G., Mari, A., Giovannetti, V.: Optimal quantum state discrimination via nested binary measurements. *Phys. Rev. A - At. Mol. Opt. Phys.* **95**(4), 1–10 (2017) [arXiv:1701.02233](https://arxiv.org/abs/1701.02233). <https://doi.org/10.1103/PhysRevA.95.042307>
- [34] Nair, R., Guha, S., Tan, S.H.: Realizable receivers for discriminating coherent and multicopy quantum states near the quantum limit. *Phys. Rev. A - At. Mol. Opt. Phys.* **89**(3), 1–9 (2014) [arXiv:1212.2048](https://arxiv.org/abs/1212.2048). <https://doi.org/10.1103/PhysRevA.89.032318>
- [35] Takeoka, M., Guha, S.: Capacity of optical communication in loss and noise with general quantum gaussian receivers. In: 2014 IEEE International Symposium on Information Theory, pp. 2799–2803 (2014). <https://doi.org/10.1109/ISIT.2014.6875344>
- [36] Bilkis, M., Rosati, M., Yepes, R.M., Calsamiglia, J.: Real-time calibration of coherent-state receivers: Learning by trial and error. *Phys. Rev. Res.* **2**(3), 033295 (2020) [arXiv:2001.10283](https://arxiv.org/abs/2001.10283). <https://doi.org/10.1103/PhysRevResearch.2.033295>
- [37] Holevo, A.S.: Gaussian Maximizers for Quantum Gaussian Observables and Ensembles. *IEEE Trans. Inf. Theory* **66**(9), 5634–5641 (2020) [arXiv:1908.03038](https://arxiv.org/abs/1908.03038). <https://doi.org/10.1109/TIT.2020.2987789>
- [38] Pedro, J., Costa, N., Pato, S.: Optical transport network design beyond 100gbaud [invited]. *Journal of Optical Communications and Networking* **12**(2), 123–134 (2020). <https://doi.org/10.1364/JOCN.12.00A123>
- [39] Sakr, H., Bradley, T.D., Hong, Y., Jasion, G.T., Hayes, J.R., Kim, H., Davidson, I.A., Fokoua, E.N., Chen, Y., Bottrill, K.R.H., Taengnoi, N., Petropoulos, P., Richardson, D.J., Poletti, F.: Ultrawide bandwidth hollow core fiber for interband short reach data transmission. In: Optical Fiber Communication Conference Postdeadline Papers 2019, pp. 4–1. Optica Publishing Group, ??? (2019). <https://doi.org/10.1364/OFC.2019.Th4A.1>. <http://opg.optica.org/abstract.cfm?URI=OFC-2019-Th4A.1>
- [40] Saleh, A.A.M., Simmons, J.M.: All-optical networking - evolution, benefits, challenges, and future vision. *Proceedings of the IEEE* **100**(5),

- 1105–1117 (2012). <https://doi.org/10.1109/JPROC.2011.2182589>
- [41] Rosati, M., Mari, A., Giovannetti, V.: Narrow Bounds for the Quantum Capacity of Thermal Attenuators. *Nat. Commun.* **9**(1), 4339 (2018) [arXiv:1801.04731](https://arxiv.org/abs/1801.04731). <https://doi.org/10.1038/s41467-018-06848-0>
- [42] Wolf, M.M., Pérez-García, D., Giedke, G.: Quantum capacities of bosonic channels. *Phys. Rev. Lett.* **98**, 130501 (2007). <https://doi.org/10.1103/PhysRevLett.98.130501>
- [43] Fanizza, M., Kianvash, F., Giovannetti, V.: Estimating Quantum and Private Capacities of Gaussian Channels via Degradable Extensions. *Phys. Rev. Lett.* **127**(21), 210501 (2021). <https://doi.org/10.1103/PhysRevLett.127.210501>
- [44] Wilde, M.M., Hayden, P., Guha, S.: Information trade-offs for optical quantum communication (2012) [arXiv:1206.4886](https://arxiv.org/abs/1206.4886). <https://doi.org/10.1103/PhysRevLett.108.140501>
- [45] Essiambre, R.-J., Kramer, G., Winzer, P.J., Foschini, G.J., Goebel, B.: Capacity limits of optical fiber networks. *Journal of Lightwave Technology* **28**(4), 662–701 (2010). <https://doi.org/10.1109/JLT.2009.2039464>
- [46] Cho, J., Chen, X., Raybon, G., et al.: Shaping lightwaves in time and frequency for optical fiber communication. *Nature Communications* **13**(785) (2022). <https://doi.org/10.1038/s41467-022-28349-x>
- [47] Mitra, P., Stark, J.: Nonlinear limits to the information capacity of optical fibre communications. *Nature* **411**, 1027–1030 (2001). <https://doi.org/10.1038/35082518>
- [48] Li, S.-A., Huang, H., Pan, Z., Yin, R., Wang, Y., Fang, Y., Zhang, Y., Bao, C., Ren, Y., Li, Z., Yue, Y.: Enabling technology in high-baud-rate coherent optical communication systems. *IEEE Access* **8**, 111318–111329 (2020). <https://doi.org/10.1109/ACCESS.2020.3003331>
- [49] Wilde, M.M.: *Quantum Information Theory*. Cambridge University Press, Cambridge (2013). <https://doi.org/10.1017/CBO9781139525343>. <http://arxiv.org/abs/1106.1445> <http://ebooks.cambridge.org/ref/id/CBO9781139525343>